Toxicological appraisal of the chemical fractions of ambient fine (PM2.5-0.3) and quasi-ultrafine (PM0.3) particles in human bronchial epithelial BEAS-2B cells

Ghidaa Badran, Anthony Verdin, Céline Grare, Imane Abbas, Djamal Achour, Frédéric Ledoux, Mohamad Roumie, Fabrice Cazier, Dominique Courcot, Jean-Marc Lo Guidice, et al.

TOXICOLOGICAL APPRAISAL OF THE CHEMICAL FRACTIONS OF AMBIENT FINE ($PM_{2.5-0.3}$) AND QUASI-ULTRAFINE ($PM_{0.3}$) PARTICLES IN HUMAN BRONCHIAL EPITHELIAL BEAS-2B CELLS

Ghidaa BADRAN[1,2,3], Anthony VERDIN[1], Céline GRARE[2], Imane ABBAS[3], Djamal ACHOUR[2], Frédéric LEDOUX[1], Mohamad ROUMIE[3], Fabrice CAZIER[4], Dominique COURCOT[1], Jean-Marc LO GUICIDE[2], Guillaume GARÇON[2,*]

[1] Unité de Chimie Environnementale et Interactions sur le Vivant, UCEIV-EA 4492, FR CNRS 3417, Univ. Littoral Côte d'Opale, Dunkerque, France

[2] CHU Lille, Institut Pasteur de Lille, ULR 4483-IMPacts de l'Environnement Chimique sur la Santé (IMPECS), Univ. Lille, Lille, France

[3] Lebanese Atomic Energy Commission – NCSR, Beirut, Lebanon

[4] Centre Commun de Mesures, Maison de la Recherche en Environnement Industriel, Univ. du Littoral Côte d'Opale, Dunkerque, France

[*] Corresponding author: Guillaume GARÇON, IMPact de l'Environnement Chimique sur la Santé (IMPECS), Institut Pasteur de Lille, CHU Lille, Univ. Lille, Lille, France; E-mail: guillaume.garcon@univ-lille.fr

ABSTRACT

New toxicological research is still urgently needed to improve the current knowledge about the induction of some underlying mechanisms of toxicity by the different chemical fractions of ambient particulate matter (PM). This *in vitro* study sought also to better evaluate and compare the respective toxicities of fine particles ($PM_{2.5-0.3}$) and their inorganic and organic chemical fractions, and the respective toxicities of the organic chemical fractions of $PM_{2.5-0.3}$ and quasi-ultrafine particles ($PM_{0.3}$). Human bronchial epithelial BEAS-2B cells were also exposed for 6 to 48 h to relatively low doses of $PM_{2.5-0.3}$ and their organic extractable ($OEM_{2.5-0.3}$) and non-extractable ($NEM_{2.5-0.3}$) fractions, and the organic extractable fraction ($OEM_{0.3}$) of $PM_{0.3}$. We reported that not only $PM_{2.5-0.3}$, but also, to a lesser extent, its inorganic chemical fraction, $NEM_{2.5-0.3}$, and organic chemical fraction, $OEM_{2.5-0.3}$, were able to significantly induce ROS overproduction and oxidative damage notwithstanding the early activation of NRF2 signaling pathway. Moreover, for any exposure, inflammatory and apoptotic events were noticed. Similar results were observed in BEAS-2B cells exposed to $OEM_{0.3}$, rich of polycyclic aromatic hydrocarbons and their nitrated and oxygenated derivatives. In BEAS-2B cells exposed for 24 and 48 h to $OEM_{2.5-0.3}$ and $OEM_{0.3}$, to a higher extent, there was an alteration of the levels of some critical proteins even though crucial for the autophagy rather than a real reduction of autophagy. It is noteworthy that the toxicological effects were equal or mostly higher in BEAS-2B cells exposed for 6 and/or 24 h to $PM_{2.5-0.3}$ from those exposed to $NEM_{2.5-0.3}$ or $OEM_{2.5-0.3}$, and in BEAS-2B cells exposed for 6 and/or mostly 24 h to $OEM_{0.3}$ from those exposed to $OEM_{2.5-0.3}$. Taken together, these results revealed the higher potentials for toxicity, closely linked to their respective physical and chemical characteristics, of $PM_{2.5-0.3}$ vs $NEM_{2.5-0.3}$ and/or $OEM_{2.5-0.3}$, and $OEM_{0.3}$ vs $OEM_{2.5-0.3}$.

CAPSULE: Inorganic and organic chemical fractions from ambient fine and ultrafine particles differentially triggered some critical underlying mechanisms of toxicity in BEAS-2B cells.

KEYWORDS: Fine particles; quasi-ultrafine particles; extractable and non-extractable chemical fractions; normal human bronchial epithelial BEAS-2B cells; toxicity; underlying mechanisms

INTRODUCTION

Epidemiological evidence supported the association between exposure to ambient particulate matter (PM) and hospital admissions, morbidity and mortality related to chronic inflammatory lung diseases (e.g., asthma and chronic obstructive pulmonary disease) and lung cancer (Beelen et al. 2013; Doiron et al. 2019; Hamra et al. 2014; Jerrett et al. 2016; Lelieveld et al. 2019; Raaschou-Nielsen et al. 2016; Loomis et al. 2014). Fine (i.e., $PM_{2.5}$) and mostly ultrafine (i.e., $PM_{0.1}$) particles have generally been reported as the major contributors to the adverse health effects of air pollution (Abbas et al. 2018). Several experimental studies have notified the harmful lung effects of ambient PM, mostly through their ability to trigger some critical underlying mechanisms of toxicity, such as oxidative stress-induced airway inflammation (e.g., Abbas et al. 2013, 2016, 2019; Bocchi et al. 2016; Garçon et al. 2006; Gualtieri et al. 2010, 2011; Halonen et al. 2015; Leclercq et al. 2016, 2017, 2018; Longhin et al. 2013, 2016, Sotty et al. 2019). However, although significant progress has been made during the last decade, a considerable effort will continue to be required to better identify some typical features of *in vitro* toxicological responses, which could be related to some of the specific physical and chemical characteristics of ambient PM.

A careful consideration has already been devoted to the types of toxicological responses induced by ambient PM, since their knowledge is greatly complicated by the fact that it is a very heterogeneous and often poorly described pollutant (Perrone et al. 2013). Despite the particular attention of the scientific community about the types of toxicological responses depending on the sources of ambient PM, this question is still far from being completely resolved. Gualtieri et al. (2010), Lonkar and Dedon (2011), and Perrone et al. (2013) have all used the inclusion of the grouping of inorganic constituents to provide useful information on the differential effects of the

components and/or the sources of ambient PM. Hence, it is worthy to extend this approach to organic components. Among them, polycyclic aromatic hydrocarbons (PAH) were identified as major redox-active components, which, through their metabolic activation into highly biologically reactive electrophile metabolites, largely contribute to the overall toxicity of ambient PM (Abbas et al., 2018; Boublil et al. 2013; Longhin et al. 2013, 2016; Sotty et al. 2019; Zhou et al. 2016). Oher authors reported the critical role of the organic extractable matter (OEM) derived from ambient PM in its overall toxicity but failed to fully clarify them (Akhtar et al. 2010; Alessandria et al. 2014; De Brito et al. 2013, Oh et al. 2011, Xiang et al. 2018).

New toxicological research is therefore requested to improve the current knowledge about the specific involvement of the inorganic and organic chemical fractions of ambient PM in its overall toxicity. Recently, OEM derived from ambient $PM_{2.5-0.3}$ was recognized as triggering oxidative, inflammatory, and genotoxic events: a combination thereof may be the same or different in comparison with those triggered by the whole $PM_{2.5-0.3}$. However, further works are still needed to better compare the respective roles of each chemical fraction: it might also be more appropriate to study the toxicity of $OEM_{2.5-0.3}$ together with this of the whole $PM_{2.5-0.3}$, from which it was extracted, and the toxicity of non-extractable matter ($NEM_{2.5-0.3}$; i.e., residual $PM_{2.5-0.3}$ after $OEM_{2.5-0.3}$ extraction). The comparison between the specific toxicities of $OEM_{2.5-0.3}$ and $OEM_{0.3}$, respectively prepared from fine ($PM_{2.5-0.3}$) or quasi-ultrafine ($PM_{0.3}$) particles, could also be very interesting to better assess the chemical compounds mainly involved. Hence, in this work, we sought to better investigate: (i) the toxicological effects of $OEM_{2.5-0.3}$ and $NEM_{2.5-0.3}$ with a particular attention being paid to oxidative, inflammatory, autophagic, and apoptotic events, and thereafter compare them to those of $PM_{2.5-0.3}$ in its entirety, and (ii) the toxicity of $OEM_{0.3}$ which would lastly be related to that of $OEM_{2.5-0.3}$.

MATERIALS AND METHODS

Chemicals

Sigma-Aldrich (Saint-Quentin Fallavier, France) provided BEAS-2B cells (ATCC® CRL-9609™) and chemicals. ThermoFisher scientific (Villebon-sur-Yvette, France) provided hydro-ethidium (HE), 6-carboxy-2',7'-dichlorodihydrofluorescein diacetate (carboxy-H2DCFDA), Pierce™ BCA protein assay kits, Click-iT™ Plus EdU Alexa Fluor™ 647 flow cytometry assay kits, Single-channel dead cell apoptosis kits with Annexin V alexa fluor™ 488, and SYTOX™ green dyes, and other biological reagents. Qiagen (Courtaboeuf, France) provided RNeasy mini Kits. Promega (Charbonnière-les-Bains, France) provided CellTiter-Glo® luminescent cell viability, GSH/GSSG-Glo™ assay, and Caspase Glo® 3/7, Caspase Glo® 8, and Caspase Glo® 9 assays. Gentaur (Paris, France) provided Highly sensitive 8-OHdG check kits. Abcam (Cambridge, UK) provided Protein carbonyl content assay kits and 8-isoprostane ELISA kits. Active Motif (La Hulpe, Belgium) provided Nuclear extract and TransAM® NRF2 kits. Merck-Millipore (St Quentin-en-Yvelines, France) provided MILLIPLEX® MAP human cytokine/chemokine magnetic bead panel-immunology multiplex assays. Bio-techne (Rennes, France) provided TACS® TdT *in situ*-fluorescein system and mouse monoclonal anti-human actin antibody (MAB8929), rabbit polyclonal anti-human ATG5 (NB110-53818), rabbit polyclonal anti-human LC3-B antibody (NB100-2220), rabbit polyclonal anti-human beclin antibody (NB500-249), mouse monoclonal anti-human p62/SQSTM1 antibody (H00008878-M01), and goat polyclonal anti-rabbit IgG, HRP-linked antibody (NB7160). Cell Signaling Technology (Montigny-le-Bretonneux, France) provided rabbit monoclonal anti-mouse IgG, HRP-linked antibody (S7076).

Sampling site description, PM sampling methods, PM physicochemical characterization, and PM fraction preparation

Sampling site description, sampling procedure, physicochemical characterization of $PM_{2.5\text{-}0.3}$ and $PM_{0.3}$, and preparation of $NEM_{2.5\text{-}0.3}$, $OEM_{2.5\text{-}0.3}$, and $OEM_{0.3}$ have been published elsewhere (Badran et al. 2020; see also supplemental data: Tables S1 and S2, and Figure S1).

Cell culture and exposure

Normal human bronchial epithelial BEAS-2B cells (ATCC® CRL-9609™) were cultured as published elsewhere (Leclercq et al. 2017). Just before reaching the confluence (< 80%), BEAS-2B cells were incubated either with LHC-9 with dimethylsulfoxide (DMSO) at 0.5% (v/v), as a negative control, or with $PM_{2.5\text{-}0.3}$, $NEM_{2.5\text{-}0.3}$, $OEM_{2.5\text{-}0.3}$, and $OEM_{0.3}$, prepared in LHC-9 with DMSO ≤ 0.5% (v/v), at concentrations ranging from 3 to 96 µg Eq. PM/cm^2, as detailed elsewhere (Badran et al. 2020). Aliquots of cell-free culture supernatants were collected after 6, 24 and/or 48 h, and quickly frozen at -80°C. Adherent cells were washed twice with 1 mL-aliquots of cold sterile PBS, and either immediately fixed or quickly frozen at -80°C, as published elsewhere (Sotty et al. 2019).

Cytotoxicity

Intracellular ATP concentrations of BEAS-2B cells were determined using the CellTiter-Glo® luminescent cell viability (Promega). This assay system used the properties of a proprietary thermostable luciferase to enable reaction conditions that generate a stable "glow-type" luminescent signal. The mono-oxygenation of luciferin was catalyzed by luciferase in the presence

of Mg^{2+}, ATP, and molecular oxygen, and resulted in the emission of light, directly linked to the ATP concentration and also the number of living cells.

Oxidative stress

Firstly, the fluorescence of either HE (1 µM) or carboxy-H_2DCFDA (1 µM) was kinetically monitored at 37°C within BEAS-2B cells. Secondly, the nuclear factor erythroid 2-related factor 2 (NRF2) DNA binding activity was studied using TransAM® NRF2 from Active Motif. Associated gene expressions of some members of the NRF2 signaling pathway (i.e., *NRF2; Kelch-like ECH-associated protein 1, KEAP-1; heme oxygenase 1, HMOX; NAD(P)H quinone dehydrogenase 1, NQO1; superoxide dismutase, SOD)* were evaluated by RT-qPCR using specific Taqman™ gene expression assays (*NRF2*: hs00975961_g1, *KEAP-1*: hs00202227_m1, *HMOX*: Hs01110250_m1, *NQO1*: Hs01045993_g1, *SOD*: hs00162090_m1, *ARN18S*: Hs99999901_s1), a StepOnePlus™ Real-Time PCR System, and the Expression Suite Software (ThermoFisher scientific). Thirdly, the status of glutathione (GSSG/GSH), and the concentrations of carbonylated protein (CO-protein), 8-isoprostane (8-Isop), and 8-hydroxy-2'-deoxyguanosine (8-OHdG) were carried out using GSH/GSSG-Glo™ assay (Promega), Protein carbonyl content assay kits (Abcam), 8-isoprostane ELISA kits (Abcam), and Highly sensitive 8-OHdG check enzyme immunoassays (Gentaur), respectively, as published elsewhere (Leclercq et al. 2016). Menadione (2.5 mM, 4 h)-treated BEAS-2B cells served as a positive control.

Inflammation

The secretion of tumor necrosis factor (TNF-α), interleukin-6 (IL-6), interleukin-8 (IL-8), and monocyte chemoattractant protein 1 (MCP-1) in the cell-free culture supernatants of BEAS-2B

cells was detected by MILLIPLEX® MAP Human Cytokine/Chemokine Magnetic Bead Panel-Immunology Multiplex Assay (Merck-Millipore). Lipopolysaccharide (LPS from E. coli, 50 µg/mL, 24 h)-treated BEAS-2B cells served as a positive control.

Autophagy

ATG5, BECN1/Beclin 1, SQSTM1/p62 protein, and microtubule-associated protein 1 light chain 3 b (MAP1LC3B/LC3B) were studied within BEAS-2B cells. Protein extracts (20 µg) of BEAS-2B cells were prepared using protease and phosphatase inhibitor cocktail (Sigma-Aldrich)-supplemented RIPA lysis/extraction buffer (ThermoFisher scientific). Western-blot method consisted of: separation by electrophoresis on SDS-PAGE gels, transfer on nitrocellulose membranes, blockage in 5 % (m/v) non-fat dry milk for 45 min, primary antibody incubation overnight at +4°C (i.e., rabbit polyclonal anti-human ATG5, rabbit polyclonal anti-human LC3-B antibody, rabbit polyclonal anti-human Beclin antibody, mouse monoclonal anti-human p62/SQSTM1 antibody, mouse monoclonal anti-human actin antibody (Bio-techne), secondary antibody incubation for 1 h at room temperature (i.e., rabbit monoclonal anti-mouse IgG, HRP-linked antibody, Cell Signaling Technology; goat polyclonal anti-rabbit IgG, HRP-linked antibody, Bio-techne), and revelation by ECL prime Western Blotting Detection reagent (GE Healthcare). Chemiluminescence was recorded by Fusion FX Spectra (Vilbert-Lourmat, Marne-la-Vallée, France). Rapamycine (10 µM, 24 h)-treated BEAS-2B cells served as a positive control.

Apoptosis

Caspase Glo® 3/7, Caspase Glo® 8, and Caspase Glo® 9 Assays (Promega) were used as recommended by the manufacturer. TACS® TdT *in situ*-Fluorescein System (Bio-techne) was

191 used according to the manufacturer's recommendations before BEAS-2B cell observations using
192 an EVOS® FL Cell Imaging System (ThermoFisher scientific). Single-channel dead cell apoptosis
193 kit with Annexin V Alexa Fluor™ 488 and SYTOX™ green dyes, and Click-iT™ Plus EdU Alexa
194 Fluor™ 647 flow cytometry assay kits (ThermoFisher scientific) were used as recommended by
195 the manufacturer, before BEAS-2B cell analysis using an Attune™ NxT Acoustic Focusing
196 Cytometer (ThermoFisher scientific) to study apoptosis and cell cycle, respectively. Staurosporine
197 (2.5 µM, 24 h)-treated BEAS-2B cells served as a positive control.
198
199 **Statistical analysis**
200 Results were expressed as mean values and standard deviations. Comparisons were performed
201 between data from exposed BEAS-2B cells (i.e., $PM_{2.5\text{-}0.3}$, $NEM_{2.5\text{-}0.3}$ $OEM_{2.5\text{-}0.3}$, or $OEM_{0.3}$) and
202 those from negative controls. Significant differences between results from BEAS-2B cells exposed
203 either to $NEM_{2.5\text{-}0.3}$ or $OEM_{2.5\text{-}0.3}$ vs $PM_{2.5\text{-}0.3}$, and to $OEM_{0.3}$ vs $OEM_{2.5\text{-}0.3}$ were reported. The non-
204 parametric Mann-Whitney U-test with correction for multiple comparisons ($p < 0.05$) was used to
205 perform statistical analyses (Software: SPSS for windows).
206

RESULTS AND DISCUSSION

$PM_{2.5-0.3}$, $NEM_{2.5-0.3}$, $OEM_{2.5-0.3}$, and $OEM_{0.3}$-induced cytotoxicity

As shown in Figure S2 (see also supplemental data), significant decreases of intracellular ATP concentrations were reported in BEAS-2B cells 6, 24 and 72 h after their exposure to $PM_{2.5-0.3}$, from the dose of 6 µg/cm^2. Almost a similar profile of intracellular ATP concentrations was seen in BEAS-2B cells after their exposure to $NEM_{2.5-0.3}$. In contrast, both $OEM_{2.5-0.3}$ and particularly $OEM_{0.3}$ significantly altered intracellular ATP concentrations of BEAS-2B cells only for the highest doses, almost since 48 µg Eq. PM/cm². The dose- and/or time-dependent cytotoxicity of $PM_{2.5-0.3}$, $NEM_{2.5-0.3}$, $OEM_{2.5-0.3}$, and $OEM_{0.3}$ observed in BEAS-2B cells allowed to choose the concentrations (i.e., 3 and 12 µg Eq. PM/cm²) and kinetic (from 6 to 48 h) to apply to the further study of the other toxicological endpoints. It is noteworthy that both these concentrations were among the lowest shown as toxicologically active without, however, triggering massive regulated cell death (RCD) (Abbas et al. 2019; Badran et al., 2020; Gualtieri et al. 2010, 2011; Leclercq et al. 2018; Longhin et al., 2013, 2016; Platel et al. 2019; Sotty et al. 2019).

$PM_{2.5-0.3}$, $NEM_{2.5-0.3}$, $OEM_{2.5-0.3}$, and $OEM_{0.3}$-induced oxidative stress

Oxidative stress is one of the primary critical underlying mechanisms of toxicity activated by the inhalation of ambient PM. A ROS overproduction by the BEAS-2B cells 6 and 24 h after their exposures to $PM_{2.5-0.3}$, $NEM_{2.5-0.3}$, $OEM_{2.5-0.3}$, or $OEM_{0.3}$ was shown in Figure 1. Indeed, HE fluorescence intensity increased in a dose-dependent manner in BEAS-2B cells 6 and 24 h after their exposures to $NEM_{2.5-0.3}$ and $OEM_{2.5-0.3}$, and more markedly $PM_{2.5-0.3}$ and $OEM_{0.3}$ (Figure 1-

A, B). It is noteworthy that, after 6 and 24 h, HE fluorescence was significantly higher in BEAS-2B cells exposed to $PM_{2.5\text{-}0.3}$ from those exposed to $NEM_{2.5\text{-}0.3}$ or $OEM_{2.5\text{-}0.3}$, and in BEAS-2B cells exposed to $OEM_{0.3}$ from those exposed to $OEM_{2.5\text{-}0.3}$. Carboxy-H_2DCFDA fluorescence revealed almost similar changes (Figure 1-C, D). The ahead-reported intracellular overproduction of ROS in BEAS-2B cells could be related either to the inorganic chemicals (e.g., Al, Cr, Cu, Fe, Mn, Ni, Pb, Ti, and Zn) detected within $PM_{2.5\text{-}0.3}$ and $NEM_{2.5\text{-}0.3}$, or to the organic chemicals (i.e., PAH, O-PAH, and N-PAH) found within $PM_{2.5\text{-}0.3}$, $OEM_{2.5\text{-}0.3}$, and rather $OEM_{0.3}$, also usually associated with redox reactions (Abbas et al. 2019, Badran et al. 2020; Gualtieri et al. 2011, Leclercq et al. 2018; Longhin et al. 2013, Oh et al. 2011, Saint-Georges et al. 2008, 2009). Accordingly, due to the presence of both inorganic and organic chemical fractions within the whole $PM_{2.5\text{-}0.3}$, there was also a higher ROS overproduction in BEAS-2B cells exposed to $PM_{2.5\text{-}0.3}$ from those exposed only to $NEM_{2.5\text{-}0.3}$ or $OEM_{2.5\text{-}0.3}$. Interestingly, the higher ROS overproduction reported in BEAS-2B cells exposed to $OEM_{0.3}$ from those exposed to $OEM_{2.5\text{-}0.3}$ could be explained by its higher contents of total carbon, PAH, O-PAH, and N-PAH (Badran et al. 2020, see also supplemental data: Figure 1, Tables S1 and S2).

In addition, significant increases of the gene expression and binding activity of NRF2 were reported in BEAS-2B cells exposed to $NEM_{2.5\text{-}0.3}$ or $OEM_{2.5\text{-}0.3}$, and more markedly to $PM_{2.5\text{-}0.3}$ or $OEM_{0.3}$ (Figure 1-E, F, G, H). All these changes were generally higher at 6 than 24 h. NRF2, because of its crucial function as a primary regulator of cellular redox homeostasis, is devoted to counteract the cytosolic overproduction of ROS and, therefore, to maintain redox balance within the cell (Wardyn et al. 2015). However, 24 h after any exposure, there was only a relatively low activation of NRF2 transcription factor, which could be explained by its possible relocalization, binding inactivation or degradation (Leclercq et al. 2018). It is important to note that, according to

ROS overproduction, the activation of the NRF2 signaling pathway was significantly higher in BEAS-2B cells exposed for 6 and 24 h to $PM_{2.5\text{-}0.3}$ from those exposed to $NEM_{2.5\text{-}0.3}$ or $OEM_{2.5\text{-}0.3}$, and in BEAS-2B cells exposed for 6 h to $OEM_{0.3}$ from those exposed to $OEM_{2.5\text{-}0.3}$ (Figure 2). Once again, all these results underlined the higher toxicity potentials of $PM_{2.5\text{-}0.3}$ vs $NEM_{2.5\text{-}0.3}$ and/or $OEM_{2.5\text{-}0.3}$, and $OEM_{0.3}$ vs $OEM_{2.5\text{-}0.3}$, also closely linked to their respective physical and chemical characteristics.

Remarkably, for any exposure, despite the early activation of NRF2 signaling pathway, oxidative alterations of glutathione, DNA and proteins significantly occurred in a dose- and time-dependent manner (Figure 3). Overall, the highest oxidative damage to target macromolecules was reported in BEAS-2B cells 24 h after their exposures to $PM_{2.5\text{-}0.3}$, and interestingly $OEM_{0.3}$ rather than $NEM_{2.5\text{-}0.3}$ and $OEM_{2.5\text{-}0.3}$, thereby underlining the higher toxicity potentials of $PM_{2.5\text{-}0.3}$ vs $NEM_{2.5\text{-}0.3}$ and/or $OEM_{2.5\text{-}0.3}$, and $OEM_{0.3}$ vs $OEM_{2.5\text{-}0.3}$. Overall, these results supported the occurrence of a remarkable cytosolic oxidative stress in BEAS-2B cells after their exposures to $PM_{2.5\text{-}0.3}$ and $OEM_{0.3}$, and $NEM_{2.5\text{-}0.3}$ and $OEM_{2.5\text{-}0.3}$, to a lesser extent, and the inability of the NRF2 signaling pathway to totally counteract ROS overproduction. Oxidative damage to DNA, proteins and/or lipids can also disrupt the cell homeostasis, thereby contributing to gene expression deregulation, DNA mutation, protein alteration with loss of function, and lipid peroxidation with loss of membrane integrity and/or fluidity (Abbas et al. 2019; Dergham et al., 2012, 2015; Garçon et al., 2006; Gualtieri et al., 2010, 2011; Leclercq et al. 2016, 2017, 2018; Longhin et al. 2013, 2016).

$PM_{2.5\text{-}0.3}$, $NEM_{2.5\text{-}0.3}$, $OEM_{2.5\text{-}0.3}$, and $OEM_{0.3}$-induced cytokine secretion

275 The four cytokines under study, TNF-α, IL-6, IL-8 and MCP-1, were significantly secreted
276 by BEAS-2B cells 6 and 24 h after their exposures to $PM_{2.5-0.3}$, and $NEM_{2.5-0.3}$, to a lesser extent,
277 but only 6 h after their exposure to $OEM_{2.5-0.3}$, and $OEM_{0.3}$ (Figure 4). Once again, except for TNF-
278 α, the highest concentrations of the three other cytokines have been secreted by BEAS-2B cells
279 exposed for 24 h to $PM_{2.5-0.3}$ from those exposed to $NEM_{2.5-0.3}$ and/or $OEM_{2.5-0.3}$ (Figure 4-D, F,
280 H). In keeping with the current literature, a significant secretion of proinflammatory cytokines by
281 BEAS-2B cells or other lung cell models, acutely or repeatedly exposed to relatively low doses of
282 ambient PM, has already been reported (Abbas et al. 2019; Dergham et al., 2012, 2015; Boulbil et
283 al. 2013; Garçon et al., 2006; Ghio et al. 2013; Gualtieri et al. 2010, 2011; Leclercq et al. 2016,
284 2018; Longhin et al. 2013, 2016; Loxham et al. 2015; Sotty et al. 2019; Zhou et al. 2016). The
285 relationship between the contents of redox-active compounds in ambient PM and the secretion of
286 proinflammatory cytokines by lung cells might closely rely on the regulation of NF-κB (Lodovici
287 and Bigagli, 2011).
288 However, in this work, despite the significant secretion of these cytokines by BEAS-2B cells
289 exposed for 6 h to $OEM_{2.5-0.3}$ and $OEM_{0.3}$, no significant secretion of them was still observed after
290 24 h. Interestingly, other authors, contributing to better decipher the underlying mechanisms of
291 toxicity of PAH-rich PM in different mouse or human cell models reported a negative association
292 between the PAH contents of ambient PM and the secretion of inflammatory cytokines (Jalava et
293 al. 2009; Kaur et al., 2019; Manzano-León et al. 2016).
294 Moreover, although the endotoxin contents have not been determined in $PM_{2.5-0.3}$, $PM_{0.3}$, nor
295 their NEM nor OEM, their possible influences on the secretion of the proinflammatory mediators
296 could not be excluded.

297 Another explanation supporting the difference between the results arising from cells exposed
298 to metal-rich PM ($PM_{2.5\text{-}0.3}$ and $NEM_{2.5\text{-}0.3}$) vs PAH-rich PM ($OEM_{2.5\text{-}0.3}$ and $OEM_{2.5\text{-}0.3}$) in terms
299 of cytokine secretion could be related to the bioavailability and the bioaccessibility of the organic
300 compounds, whether those adsorbed-on core PM, or found in OEM (Garçon et al. 2004a, 2004b).
301 The cell absorption of native particles by endocytosis, and the vector role of core PM could also
302 facilitate the absorption of organic compounds, while PAH within OEM could be directly diluted
303 in the culture medium. At once, PAH-coated onto PM could be only progressively released in cell
304 cytoplasm after particle internalization, and progressively metabolized, thereby contributing to
305 prolong their adverse effects within target cells. In contrast, the specific chemical properties of
306 OEM, which regrouped lipophilic compounds that can easily and even rapidly go through the
307 cytoplasmic membrane and could be freely, quickly, metabolized, within the cell, could contribute
308 to shorten their adverse effects within the target cells.
309
310 **$PM_{2.5\text{-}0.3}$, $NEM_{2.5\text{-}0.3}$, $OEM_{2.5\text{-}0.3}$, and $OEM_{0.3}$-induced autophagy**
311 Mounting evidence further suggests that the autophagy machinery is closely involved in
312 extensive crosstalk with several chronic inflammatory lung diseases, including asthma and COPD,
313 and several, if not all forms of RCD, either by hyperactivation or by inhibition of the autophagy
314 flow (Racanelli et al. 2016; Napoletano et al. 2019; Zhou et al. 2016). The evaluation of some
315 hallmarks (i.e., BECN1/Beclin 1, ATG5, SQSTM1/p62 protein, and MAP1LC3B/LC3B) was also
316 undertaken to better decipher the possible alteration of the autophagy process within BEAS-2B
317 cells 24 and 48 h after their exposures to $PM_{2.5\text{-}0.3}$, $NEM_{2.5\text{-}0.3}$, $OEM_{2.5\text{-}0.3}$, or $OEM_{0.3}$ (Figure 5).
318 Significant decreases of ATG5 and Beclin1 were noted in BEAS-2B cells 24 h after their exposures
319 only to $OEM_{2.5\text{-}0.3}$ and $OEM_{0.3}$, thereby supporting the reduction of two critical proteins, even

320 though crucial for the autophagy process. Remarkably, the highest decreases of these autophagy
321 hallmarks have been observed in BEAS-2B cells exposed for 24 h to $OEM_{0.3}$ from those exposed
322 to $OEM_{2.5-0.3}$ (Figure 5-B, D). Two ubiquitin-like conjugation systems, LC3B and ATG5-12, up-
323 regulated by another critical autophagy protein, Beclin, are generally highly required prior to
324 autophagosome formation (An et al. 2019). One of the well-described hallmarks of autophagosome
325 formation consists of the conversion of LC3-I unconjugated cytosolic form to LC3-II
326 autophagosomal membrane-associated phosphatidyle-thanolamine-conjugated form.
327 Interestingly, LC3B-II/LC3B-I protein ratio appeared to be specifically reduced in BEAS-2B cells
328 only 48 h after their exposures to $OEM_{2.5-0.3}$ and mostly $OEM_{0.3}$. Overall, the alterations of these
329 critical proteins closely involved in the autophagy process revealed differential responses of whole
330 PM or NEM towards PAH-rich OEM. However, according to Yoshii and Mizushima (2017), while
331 LC3 is currently the most widely used autophagosome marker, man must keep in mind that the
332 LC3-II amount at a given time point does not necessarily estimate the autophagic activity, because
333 not only autophagy activation but also inhibition of autophagosome degradation could greatly
334 increase the amount of LC3-II. Also, LC3-II can ectopically localize on non-autophagosome
335 structures that are not turned over in the lysosome. Taken together, the present results supported
336 rather an alteration of the levels of some critical proteins even though crucial for the autophagy
337 rather than a real reduction of autophagy itself. Nevertheless, the essential role of autophagy in
338 regulating inflammation induced by PM containing environmentally persistent free radicals was
339 reported by Chen et al. (2016), and Xu et al. (2017). Their statements supported the alteration of
340 some current hallmark proteins of autophagy and at once the relatively low secretion of
341 proinflammatory cytokines, both noticed in this work in BEAS-2B cells exposed to $OEM_{2.5-0.3}$ and

342 $OEM_{0.3}$, at a higher extent, despite the absence of additional observations proving the alteration of
343 the autophagy itself.
344
345 **$PM_{2.5-0.3}$, $NEM_{2.5-0.3}$, $OEM_{2.5-0.3}$, and $OEM_{0.3}$-induced apoptosis**
346 Recent data suggested divergent cell responses towards ambient PM resulting in RCD (i.e.,
347 apoptosis, autophagy, and necrosis) (Peixoto et al. 2017). To go further, apoptosis was also
348 investigated. As depicted by Figure 6-A, B, C, the caspases 8, 9, and 7/ activities showed almost
349 similar changes in BEAS-2B cells 24 and 48 h after any exposure, thereby supporting the
350 progressive occurrence of molecular apoptotic events.
351 However, as shown by Figure 5-D, E, F, TUNEL, Annexin-V immunostaining, and cell cycle
352 phases of BEAS-2B cells, indicated rather no clear morphological characteristics of RCD, even
353 after 48 h. An et al. (2019), studying the critical interplays between oxidative stress, autophagy
354 and apoptosis induced by oxidized black carbon, noticed that it was able to activate each of them
355 in a dose-dependent manner. Other authors reported the proapoptotic effects of ambient $PM_{2.5}$
356 within different human epithelial bronchial cell models, including BEAS-2B cells (Boublil et al.
357 2013; Gualtieri et al. 2011; Leclercq et al. 2018; Longhin et al. 2013; Lee et al. 2019).
358 Peixoto et al. (2017) recently published relevant data about the relationships between the
359 exposure to ambient PM and the underlying mechanisms related to RCD, with a particular attention
360 devoted to the pivotal role played by oxidative stress in the determination of cell fate. Indeed, the
361 cellular fate was progressively directed toward RCD, and notably autophagy, when the levels of
362 ROS were overwhelming for the cells, and lead to an inhibition of the apoptotic pathway. In this
363 work, for any exposure, while no clear autophagy process has been identified, molecular but not
364 morphological evidence of apoptosis has been noted.
365

CONCLUSION

Overall, the present results clearly demonstrated that whole $PM_{2.5-0.3}$ and both its inorganic and organic chemical fractions were able to induce some underlying mechanisms of toxicity relying on ROS overproduction, inflammation, and, with regards to RCD, apoptosis rather than autophagy. Despite the capacity of $NEM_{2.5-0.3}$, and $OEM_{2.5-0.3}$ to activate them, their combination thereof may generally be lower comparing with those triggered by the whole $PM_{2.5-0.3}$. Similar data, even with equal or higher extent from those of $OEM_{2.5-0.3}$, were reported in BEAS-2B cells exposed to $OEM_{0.3}$.. Taken together, these results highlighted the higher toxicity potentials, closely linked to their physical and chemical characteristics, of the $PM_{2.5-0.3}$ vs $NEM_{2.5-0.3}$ and/or $OEM_{2.5-0.3}$, and $OEM_{0.3}$ vs $OEM_{2.5-0.3}$. Future works are still needed to go further in the better knowledge of the toxicity potentials of the different chemical fractions of ambient PM.

REFERENCES

Abbas I, Garçon G, Saint-Georges F, André V, Gosset P, Billet S, Le Goff J, Verdin A, Mulliez P, Sichel F, Shirali P (2013) Polycyclic aromatic hydrocarbons within airborne particulate matter ($PM_{2,5}$) produced DNA bulky stable adducts in a human lung cell coculture model. J Appl Toxicol 33:109-119

Abbas I, Verdin A, Escande F, Saint-Georges F, Cazier F, Mulliez P, Courcot D, Shirali P, Gosset P, Garçon G. (2016) In vitro short-term exposure to air pollution $PM_{2.5-0.3}$ induced cell cycle alterations and genetic instability in a human lung cell coculture model. Env Res. 147, 146-158.

Abbas I., Badran G., Verdin A., Ledoux F., Roumié M., Courcot D., Garçon G. (2018) Polycyclic aromatic hydrocarbon derivatives in airborne particulate matter: sources, analysis and toxicity. Environ. Chem. Lett. 16, 439–475.

Abbas I, Badran G, Verdin A, Ledoux F, Roumie M, Lo Guidice JM, Courcot D, Garçon G. (2019) In vitro evaluation of organic extractable matter from ambient $PM_{2.5}$ using human bronchial epithelial BEAS-2B cells: Cytotoxicity, oxidative stress, pro-inflammatory response, genotoxicity, and cell cycle deregulation. Environ Res. 171, 510-522.

Akhtar US, McWhinney RD, Rastogi N, Abbatt JP, Evans GJ, Scott JA. (2010) Cytotoxic and proinflammatory effects of ambient and source-related particulate matter (PM) in relation to the production of reactive oxygen species (ROS) and cytokine adsorption by particles. Inhal Toxicol. 22 Suppl 2, 37-47.

Alessandria L, Schilirò T, Degan R, Traversi D, Gilli G. (2014) Cytotoxic response in human lung epithelial cells and ion characteristics of urban-air particles from Torino, a northern Italian city. Environ Sci Pollut Res Int. 21(8), 5554-5564.

An J, Zhou Q, Wu M, Wang L, Zhong Y, Feng J, Shang Y, Chen Y. (2019) Interactions between oxidative stress, autophagy and apoptosis in A549 cells treated with aged black carbon. Toxicol In Vitro. 54, 67-74.

Badran G, Ledoux F, Verdin A, Abbas I, Roumie M, Genevray P, Landkocz Y, Lo Guidice JM, Garçon G, Courcot D. (2020). Toxicity of fine and quasi-ultrafine particles: focus on the effects of organic extractable and non-extractable matter fractions. Chemosphere 243:125440.

Beelen R, Raaschou-Nielsen O, Stafoggia M (2013) Effects of long-term exposure to air pollution on natural-cause mortality: an analysis of 22 European cohorts within the multicentre ESCAPE project. The lancet 383:785-795

Blasco H, Garçon G, Patin F, Veyrat-Durebex C, Boyer J, Devos D, Vourc'h P, Andres CR, Corcia P (2017) Panel of oxidative stress and inflammatory biomarkers in ALS: a pilot study, Can J Neurol Sci 44(1):90-95

Bocchi C, Bazzini C, Fontana F, Pinto G, Martino A, Cassoni F. (2016) Characterization of urban aerosol: seasonal variation of mutagenicity and genotoxicity of $PM_{2.5}$, PM_1 and semi-volatile organic compounds. Mutat. Res. Genet. Toxicol. Environ. Mutagen. 807, 16-23.

Boublil L, Assémat E, Borot M,C, Boland S, Martinon L, Sciare J, Baeza-Squiban A (2013) Development of a repeated exposure protocol of human bronchial epithelium *in vitro* to study the long-term effects of atmospheric particles. Toxicol in vitro 27:533-542.

Chen ZH, Wu YF, Wang PL, Wu YP, Li ZY, Zhao Y, Zhou JS, Zhu C, Cao C, Mao YY, Xu F, Wang BB, Cormier SA, Ying SM, Li W, Shen HH. (2016) Autophagy is essential forultrafine particle-induced inflammation and mucus hyperproduction in airway epithelium. Autophagy 12(2), 297-311.

de Brito KC, de Lemos CT, Rocha JA, Mielli AC, Matzenbacher C, Vargas VM. (2013) Comparative genotoxicity of airborne particulate matter ($PM_{2.5}$) using Salmonella, plants and mammalian cells. Ecotoxicol Environ Saf. 94, 14-20.

Delfino RJ, Staimer N, Tjoa T, Arhami M, Polidori A, Gillen DL, Kleinman MT, Schauer JJ, Sioutas C. (2010) Association of biomarkers of systemic inflammation with organic components and source tracers in quasi-ultrafine particles. Environ Health Perspect. 118 (6), 756-762.

Dergham M, Lepers C, Verdin A, Billet S, Cazier F, Courcot D, Shirali P, Garçon G (2012) Prooxidant and proinflammatory potency of air pollution particulate matter ($PM_{0,3-2,5}$) produced in rural- urban- or industrial surroundings in human bronchial epithelial cells (BEAS-2B). Chem Res Toxicol 25:904-919

Dergham M, Lepers C, Verdin A, Billet S, Cazier F, Courcot D, Shirali P, Garçon G (2015) Temporal-spatial variations of the physicochemical characteristics of air pollution particulate matter ($PM_{0,3-2,5}$) and toxicological effects in human bronchial epithelial cells BEAS-2B. Env Res 137:256-267

Doiron D, de Hoogh K, Probst-Hensch N, Fortier I, Cai Y, De Matteis S, Hansell AL. (2019) Air pollution, lung function and COPD: results from the population-based UK Biobank study. Eur Respir J. 54(1).

Garçon G, Gosset P, Zerimech F, Grave-Descampiaux B, Shirali P. (2004a) Effect of Fe_2O_3 on the capacity of benzo(a)pyrene to induce polycyclic aromatic hydrocarbon-metabolizing enzymes in the respiratory tract of SpragueeDawley rats. Toxicol. Lett. 150, 179e189.

445 Garçon G, Gosset P, Maunit B, Zerimech F, Creusy C, Muller J-F, Shirali P. (2004b) Influence of
446 iron ($^{56}Fe_2O_3$ or $^{54}Fe_2O_3$) in the upregulation of cytochrome P4501A1 by benzo[a]pyrene in the
447 respiratory tract of Sprague-Dawley rats. J. Appl. Toxicol. 24, 249e256.
448 Garçon G, Dagher Z, Zerimech F, Ledoux F, Courcot D, Aboukais A, Puskaric E, Shirali P (2006)
449 Dunkerque city air pollution particulate matter-induced cytotoxicity, oxidative stress and
450 inflammation in human epithelial lung cells (L132) in culture. Toxicol in vitro 20: 519-528
451 Ghio AJ, Dailey LA, Soukup JM, Stonehuerner J, Richards JH, Devlin RB (2013) Growth of
452 human bronchial epithelial cells at an air-liquid interface alters the response to particle
453 exposure. Part Fibre Toxicol 10:25
454 Gualtieri M, Øvrevik J, Holme JA, Perrone MG, Bolzacchini E, Schwarze PE, Camatini M (2010)
455 Differences in cytotoxicity versus pro-inflammatory potency of different PM fractions in
456 human epithelial lung cells, Toxicol InVitro 24:29-39
457 Gualtieri M, Ovrevik J, Mollerup S, Asare N, Longhin E, Dahlman HJ, Camatini M, Holme JA
458 (2011) Airborne urban particles (Milan winter-$PM_{2,5}$) cause mitotic arrest and cell death:
459 Effects on DNA mitochondria AhR binding and spindle organization. Mutat Res 713:18-31
460 Hamra GB, Guha N, Cohen A, Laden F, Raaschou-Nielsen O, Samet JM, Vineis P, Forastiere F,
461 Saldiva P, Yorifuji T, Loomis D (2014) Outdoor particulate matter exposure and lung cancer:
462 a systematic review and meta-analysis. Environ Health Perspect 122:906-911
463 Jalava PI, Hirvonen MR, Sillanpää M, Pennanen AS, Happo MS, Hillamo R, Cassee FR, Gerlofs-
464 Nijland M, Borm PJ, Schins RP, Janssen NA, Salonen RO. (2009) Associations of urban air
465 particulate composition with inflammatory and cytotoxic responses in RAW 246.7 cell line.
466 Inhal Toxicol. 21(12):994-1006.

467 Jerrett M, Turner MC, Beckerman BS, Pope III CA, van Donkelaar A, Martin RV, Serre M, Crouse
468 D, Gapstur SM, Krewski D, Diver WR, Coogan PF, Thurston GD, Burnett RT (2016)
469 Comparing the health effects of ambient particulate matter estimated using ground-based versus
470 remote sensing exposure estimates. Environ Health Perspect 25(4):552-559.
471 Kaur K, Jaramillo IC, Mohammadpour R, Sturrock A, Ghandehari H, Reilly C, Paine R 3rd, Kelly
472 KE. (2019) Effect of collection methods on combustion particle physicochemical properties
473 and their biological response in a human macrophage-like cell line. J Environ Sci Health A Tox
474 Hazard Subst Environ Eng. 54(12):1170-1185.
475 Leclercq B, Happillon M, Antherieu S, Hardy E,M, Alleman L,Y, Grova N, Perdrix E, Appenzeller
476 B,M, Lo Guidice J-M, Coddeville P, Garçon G (2016) Differential responses of healthy and
477 chronic obstructive pulmonary diseased human bronchial epithelial cells repeatedly exposed to
478 air pollution-derived PM_4. Env Poll 218:1074-1088
479 Leclercq B, Platel A, Antherieu S, Alleman LY, Hardy EM, Perdrix E, Grova N, Riffault V,
480 Appenzeller BM, Happillon M, Nesslany F, Coddeville P, Lo-Guidice JM, Garçon G. (2017)
481 Genetic and epigenetic alterations in normal and sensitive COPD-diseased human bronchial
482 epithelial cells repeatedly exposed to air pollution-derived $PM_{2.5}$. Environ Pollut. 230, 163-177.
483 Leclercq B, Alleman L,Y, Perdrix E, Riffault V, Happillon M, Strecker A, Lo Guidice J-M, Garçon
484 G, Coddeville P (2017) Particulate metal bioaccessibility in physiological fluids and cell culture
485 media: Toxicological perspectives? Env Res, 156:148-157
486 Leclercq B, Kluza J, Antherieu S, Sotty J, Alleman LY, Perdrix E, Loyens A, Coddeville P, Lo
487 Guidice JM, Marchetti P, Garçon G. (2018) Air pollution-derived $PM_{2.5}$ impairs mitochondrial
488 function in healthy and chronic obstructive pulmonary diseased human bronchial epithelial
489 cells. Environ Pollut. 243, 1434-1449.

490 Lee K, Lee J, Kwak M, Cho YL, Hwang B, Cho MJ, Lee NG, Park J, Lee SH, Park JG, Kim YG,
491 Kim JS, Han TS, Cho HS, Park YJ, Lee SJ, Lee HG, Kim WK, Jeung IC, Song NW, Bae KH,
492 Min JK. Two distinct cellular pathways leading to endothelial cell cytotoxicity by silica
493 nanoparticle size. J Nanobiotechnology 17(1), 24.
494 Lodovici M, Bigagli E. (2011) Oxidative stress and air pollution exposure. J Toxicol. 487074
495 Longhin E, Pezzolato E, Mantecca P, Holme J,A, Franzetti A, Camatini M, Gualtieri M (2013)
496 Season linked responses to fine and quasi-ultrafine Milan PM in cultured cells. Toxicol in vitro
497 27:551-559
498 Longhin E, Capasso L, Battaglia C, Proverbio M,C, Consentino C, Cifola I, Mangano E, Camatini
499 M, Gualtieri M (2016) Integrative transcriptomic and protein analysis of human bronchial
500 BEAS-2B exposed to seasonal urban particulate matter. Environ Poll 209:87-98
501 Lonkar, P., Dedon, P.C. (2011). Reactive species and DNA damage in chronic inflammation:
502 reconciling chemical mechanisms and biological fates. Int J Cancer. 128(9):1999-2009
503 Loomis D, Grosse Y, Lauby-Secretan B, El Ghissassi F, Bouvard V, Benbrahim-Tallaa L, Guha
504 N, Baan R, Mattock H, Straif K on behalf of the International Agency for Research on Cancer.
505 Monograph Working Group IARC, Lyon, France (2013) Lancet Oncol 14:1262-1263
506 Loxham M, Morgan-Walsh RJ, Cooper MJ, Blume C, Swindle RJ, Dennison PW, Howarth PH,
507 Cassee FR, Teagle DAH, Palmer MR, Davies DE (2015) The effects on bronchial epithelial
508 mucociliary cultures of coarse fine and ultrafine particulate matter from an underground railway
509 station. Toxicol, Sci 145(1):98-107.
510 Manzano-León N, Serrano-Lomelin J, Sánchez BN, Quintana-Belmares R, Vega E, Vázquez-
511 López I, Rojas-Bracho L, López-Villegas MT, Vadillo-Ortega F, De Vizcaya-Ruiz A, Rosas
512 Perez I, O'Neill MS, Osornio-Vargas AR. (2016) TNFα and IL-6 responses to particulate matter

513 *in vitro*: variation according to PM size, season, and polycyclic aromatic hydrocarbon and
514 soil content. Environ Health Perspect 124:406-412.
515 Napoletano F, Baron O, Vandenabeele P, Mollereau B, Fanto M. (2019) Intersections between
516 Regulated Cell Death and Autophagy. Trends Cell Biol. 29(4), 323-338.
517 Oh SM, Kim HR, Park YJ, Lee SY, Chung KH. Organic extracts of urban air pollution particulate
518 matter (PM2.5)-induced genotoxicity and oxidative stress in human lung bronchial epithelial
519 cells (BEAS-2B cells). Mutat Res. 723(2), 142-151.
520 Park M, Joo HS, Lee K, Jang M, Kim SD, Kim I, Borlaza LJS, Lim H, Shin H, Chung KH, Choi
521 YH, Park SG, Bae MS, Lee J, Song H, Park K. (2018) Differential toxicities of fine particulate
522 matters from various sources. Sci Rep. 8(1), 17007.
523 Peixoto MS, de Oliveira Galvão MF, Batistuzzo de Medeiros SR. (2017) Cell death pathways of
524 particulate matter toxicity. Chemosphere. 188, 32-48.
525 Perrone MG, Gualtieri M, Consonni V, Ferrero L, Sangiorgi G, Longhin E,Ballabio D, Bolzacchini
526 E, Camatini M. Particle size, chemical composition, seasons of the year and urban, rural or
527 remote site origins as determinants of biological effects of particulate matter on pulmonary
528 cells. Environ Pollut. 176, 215-227.
529 Peters A, Wichmann HE, Tuch T, Heinrich J, Heyder J. 1997. Respiratory effects are associated
530 with the number of ultrafine particles. Am J Respir Crit Care Med. 155(4), 1376-1383.
531 Piantadosi CA, Carraway MS, Babiker A, Suliman HB. 2008. Heme oxygenase-1 regulates cardiac
532 mitochondrial biogenesis via Nrf2-mediated transcriptional control of nuclear respiratory
533 factor-1. Circ Res. 103(11), 1232-1240.
534 Raaschou-Nielsen O, Beelen R, Wang M et al. (2016) Particulate matter air pollution components
535 and risk for lung cancer. Environ Int 87:66-73

536 Racanelli AC, Kikkers SA, Choi AMK, Cloonan SM. (2018) Autophagy and inflammation in
537 chronic respiratory disease. Autophagy 14(2), 221-232.
538 Riese DJ 2nd, Cullum RL. 2014. Epiregulin: roles in normal physiology and cancer. Semin Cell
539 Dev Biol. 28, 49-56.
540 Sotty J, Garçon G, Denayer FO, Alleman LY, Saleh Y, Perdrix E, Riffault V, Dubot P, Lo-Guidice
541 JM, Canivet L. Toxicological effects of ambient fine ($PM_{2.5-0.18}$) and ultrafine ($PM_{0.18}$) particles
542 in healthy and diseased 3D organo-typic mucocilary-phenotype models. Environ Res. 176,
543 108538.
544 Wang T, Garcia JGN, Zhang W. 2012. Epigenetic regulation in particulate matter-mediated
545 cardiopulmonary toxicities: a systems biology perspective. Curr Pharmacogenomics Person
546 Med. 10(4), 314-321.
547 Xu XC, Wu YF, Zhou JS, Chen HP, Wang Y, Li ZY, Zhao Y, Shen HH, Chen ZH. (2017)
548 Autophagy inhibitors suppress environmental particulate matter-induced airway inflammation.
549 Toxicol Lett. 280, 206-212.
550 Yoshii SR, Mizushima N. (2017) Monitoring and Measuring Autophagy. Int J Mol Sci. 18(9). pii:
551 E1865.
552 Zhou W, Tian D, He J, Wang Y, Zhang L, Cui L, Jia L, Li L, Shu Y, Yu S (2016) Repeated $PM_{2,5}$
553 exposure inhibits BEAS-2B cell P53 expression through ROS-Akt-DNMT3B pathway-
554 mediated promoter hypermethylation, Oncotarget 7:20691-20703.
555

FUNDING SOURCES

The National Council for Scientific Research of Lebanon (Grant Research Program, Ref: 04-06-2014) contributes to support he research described in this article. Both the UCEIV-EA4492 and the EA4483- IMPECS benefited from grants from the CLIMIBIO project, also supported by the Hauts-de-France Region Council, the French Ministry of Higher Education and Research, and the European Regional Development Funds.

564 **Figure Legend**
565

566 **Figure 1:** Fluorescence intensity of hydroethidium (HE) (Figure 1-A, B) and 6-carboxy-2',7'-
567 dichlorodihydrofluorescein diacetate (carboxy-H_2DCFDA) (Figure 1-C, D), and gene expression
568 and/or protein binding activity of nuclear factor erythroid 2-related factor 2 (NRF-2) (Figure 1-E,
569 F and Figure 1-G, H, respectively), 6 (Figure 1-A, C, E, G) and 24 h (Figure 1-B, D, F, H) after
570 BEAS-2B cell exposure to fine particles ($PM_{2.5-0.3}$) and their extractable ($OEM_{2.5-0.3}$) and non-
571 extractable ($NEM_{2.5-0.3}$) fractions, and to the extractable fraction ($OEM_{0.3}$) of the ultrafine particles
572 ($PM_{0.3}$). Menadione (100 µM, 4 h) was used as positive control. Results are normalized to controls
573 and presented as means and standard deviations of 6 or 3 replicates from three independent
574 experiments. (Mann-Whitney U-test; vs. controls: * = $p < 0.05$, and *** = $p < 0.001$; vs. $PM_{2.5-0.3}$
575 or vs $OEM_{0.3}$: c = $p < 0.05$).
576

577 **Figure 2:** Gene expression of Kelch-like ECH-associated protein 1 (KEAP-1) (Figure 2-A, B),
578 heme oxygenase 1 (HMOX) (Figure 2-C, D), NAD(P)H quinone dehydrogenase 1 (NQO1) (Figure
579 2-E, F), and superoxide dismutase (SOD) (Figure 2-G, H) in BEAS-2B cells, 6 (Figure 2-A, C, E,
580 G) and 24 h (Figure 2-B, D, F, H) after BEAS-2B cell exposure to fine particles ($PM_{2.5-0.3}$) and
581 their extractable ($OEM_{2.5-0.3}$) and non-extractable ($NEM_{2.5-0.3}$) fractions, and to the extractable
582 fraction ($OEM_{0.3}$) of the ultrafine particles ($PM_{0.3}$). Results are normalized to controls and
583 presented as means and standard deviations of 3 replicates from three independent experiments.
584 (Mann-Whitney U-test; vs. controls: * = $p < 0.05$; vs. $PM_{2.5-0.3}$ or vs $OEM_{0.3}$: c = $p < 0.05$).
585

586 **Figure 3:** Glutathione status (Figure 3-A, B), 8-hydroxy-2'-deoxyguanosine (8-OHdG) (Figure 3-
587 C, D), carbonylated protein (CO-protein) (Figure 3-E, F), and 8-isoprostane (8-Isop) (Figure 3-G,

588 H) in BEAS-2B cells, 6 (Figure 3-A, C, E, G) and 24 h (Figure 3-B, D, F, H) after BEAS-2B cell
589 exposure to fine particles ($PM_{2.5-0.3}$) and their extractable ($OEM_{2.5-0.3}$) and non-extractable
590 ($NEM_{2.5-0.3}$) fractions, and to the extractable fraction ($OEM_{0.3}$) of the ultrafine particles ($PM_{0.3}$).
591 Results are normalized to controls and presented as means and standard deviations of 3 replicates
592 from three independent experiments. (Mann-Whitney U-test; vs. controls: * = $p < 0.05$; vs. $PM_{2.5-0.3}$ or vs $OEM_{0.3}$: c = $p < 0.05$).
593
594
595 **Figure 4:** Concentrations of tumor necrosis factor (TNF-α) (Figure 4-A, B), interleukin-6 (IL-6)
596 (Figure 4-C, D), interleukin-8 (IL-8) (Figure 4-E, F), and monocyte chemoattractant protein-1
597 (MCP-1) (Figure 4-G, H), in BEAS-2B cells, 6 (Figure 4-A, C, E, G) and 24 h (Figure 4-B, D, F,
598 H) after BEAS-2B cell exposure to fine particles ($PM_{2.5-0.3}$) and their extractable ($OEM_{2.5-0.3}$) and
599 non-extractable ($NEM_{2.5-0.3}$) fractions, and to the extractable fraction (OEM0.3) of the ultrafine
600 particles ($PM_{0.3}$). Results are normalized to controls and presented as means and standard
601 deviations of 3 replicates from three independent experiments. Baseline cytokine secretion of
602 BEAS-2B cells for 6 and 24 h were respectively: 36 ± 14 pg/mL and 48 ± 16 pg/mL for TNF-α,
603 66 ± 20 pg/mL and 78 ± 21 pg/mL for IL-6, 410 ± 49 pg/mL and 648 ± 74 pg/mL for IL-8, and
604 973 ± 94 pg/mL and 1390 ± 173 pg/mL for MCP-1. (Mann-Whitney U-test; vs. controls: * = $p <$
605 0.05; vs. $PM_{2.5-0.3}$ or vs $OEM_{0.3}$: c = $p < 0.05$).
606
607 **Figure 5:** Protein expression of autophagy-related 5 (Figure 5-A), BECN1/Beclin 1 (Figure 5-B),
608 SQSTM1/p62 protein (Figure 5-C), and microtubule-associated protein 1 light chain 3 b
609 (MAP1LC3B/LC3B) (Figure 5-D) in BEAS-2B cells 24 and 48 h after BEAS-2B cell exposure to
610 fine particles ($PM_{2.5-0.3}$) and their extractable ($OEM_{2.5-0.3}$) and non-extractable ($NEM_{2.5-0.3}$)

611 fractions, and to the extractable fraction ($OEM_{0.3}$) of the ultrafine particles ($PM_{0.3}$) at 12 µg Eq.
612 PM/cm^2. Results are normalized to controls and presented as means and standard deviations of 3
613 replicates from three independent experiments. (Mann-Whitney U-test; vs. controls: * = $p < 0.05$;
614 vs. $PM_{2.5-0.3}$ or vs $OEM_{0.3}$: c = $p < 0.05$).
615
616 **Figure 6:** Activities of caspases 3/7, 8, and 9 (Figure 6-A, B, C, respectively),
617 immunofluorescence labelling of apoptotic cells using the TdT-mediated dUTP Nick-End
618 Labeling (TUNEL) method (Figure 6-D), detection of apoptotic cells using the Single-channel
619 dead cell apoptosis kit with Annexin V Alexa Fluor™ 488 and SYTOX™ green dyes (Figure 6-
620 F) and cell cycle analysis using Click-iT™ Plus EdU Alexa Fluor™ 647 flow cytometry assay kit
621 (Figure 6-G) in BEAS-2B cells, 24 and 48 h after BEAS-2B cell exposure to fine particles ($PM_{2.5-0.3}$)
622 and their extractable ($OEM_{2.5-0.3}$) and non-extractable ($NEM_{2.5-0.3}$) fractions, and to the
623 extractable fraction ($OEM_{0.3}$) of the ultrafine particles ($PM_{0.3}$) at 12 µg Eq. PM/cm^2. Staurosporine
624 (2.5 µM, 24 h) has been used as positive control. Results are normalized to controls and presented
625 as means and standard deviations of 3 replicates from three independent experiments. (Mann-
626 Whitney U-test; vs. controls; * = $p < 0.05$).

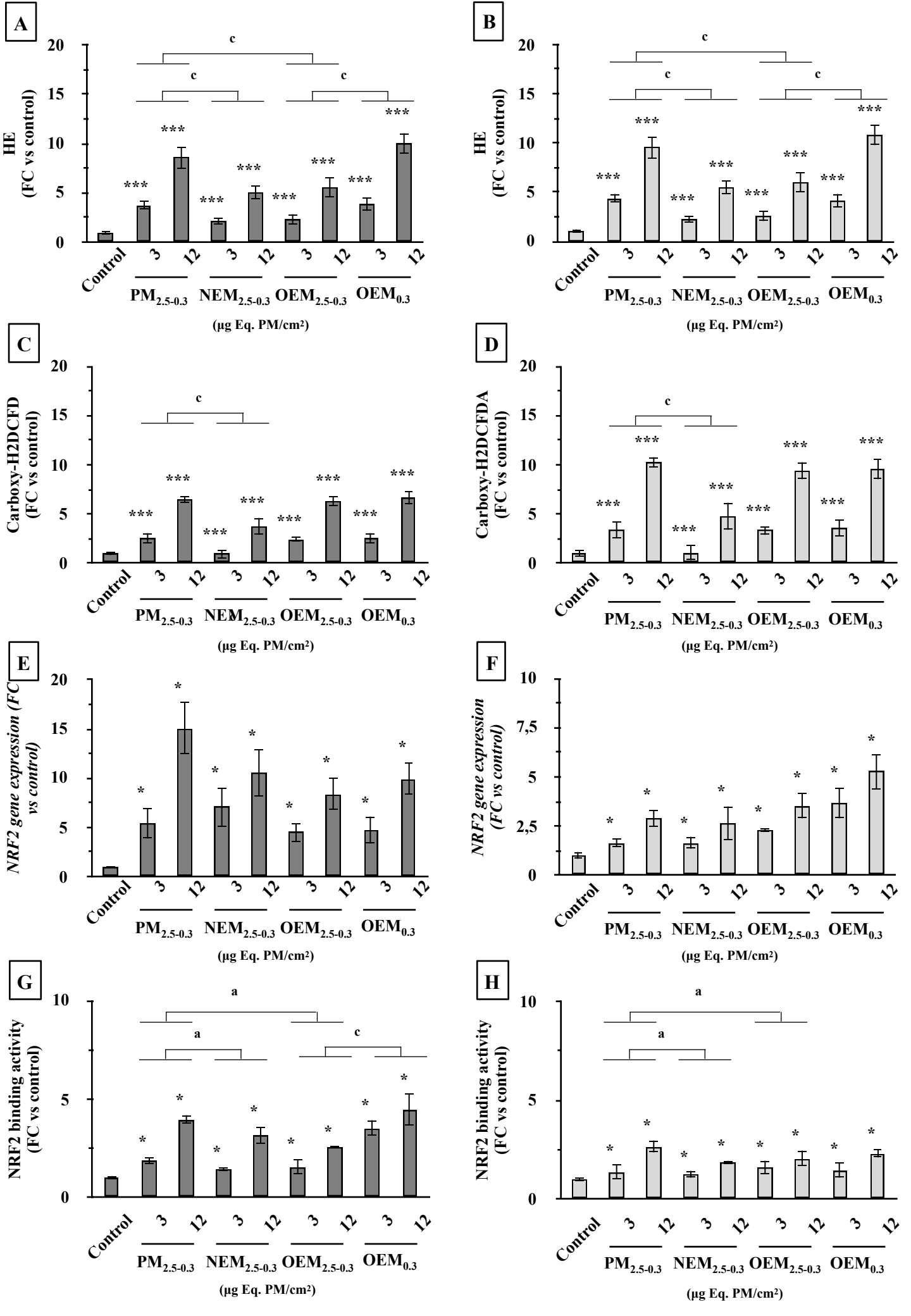
A
B
C
D
E
F
G
H
HE (FC vs control)
Carboxy-H2DCFD (FC vs control)
Carboxy-H2DCFDA (FC vs control)
NRF2 gene expression (FC vs control)
NRF2 binding activity (FC vs control)
Control
3
12
PM2.5-0.3
NEM2.5-0.3
OEM2.5-0.3
OEM0.3
(µg Eq. PM/cm²)

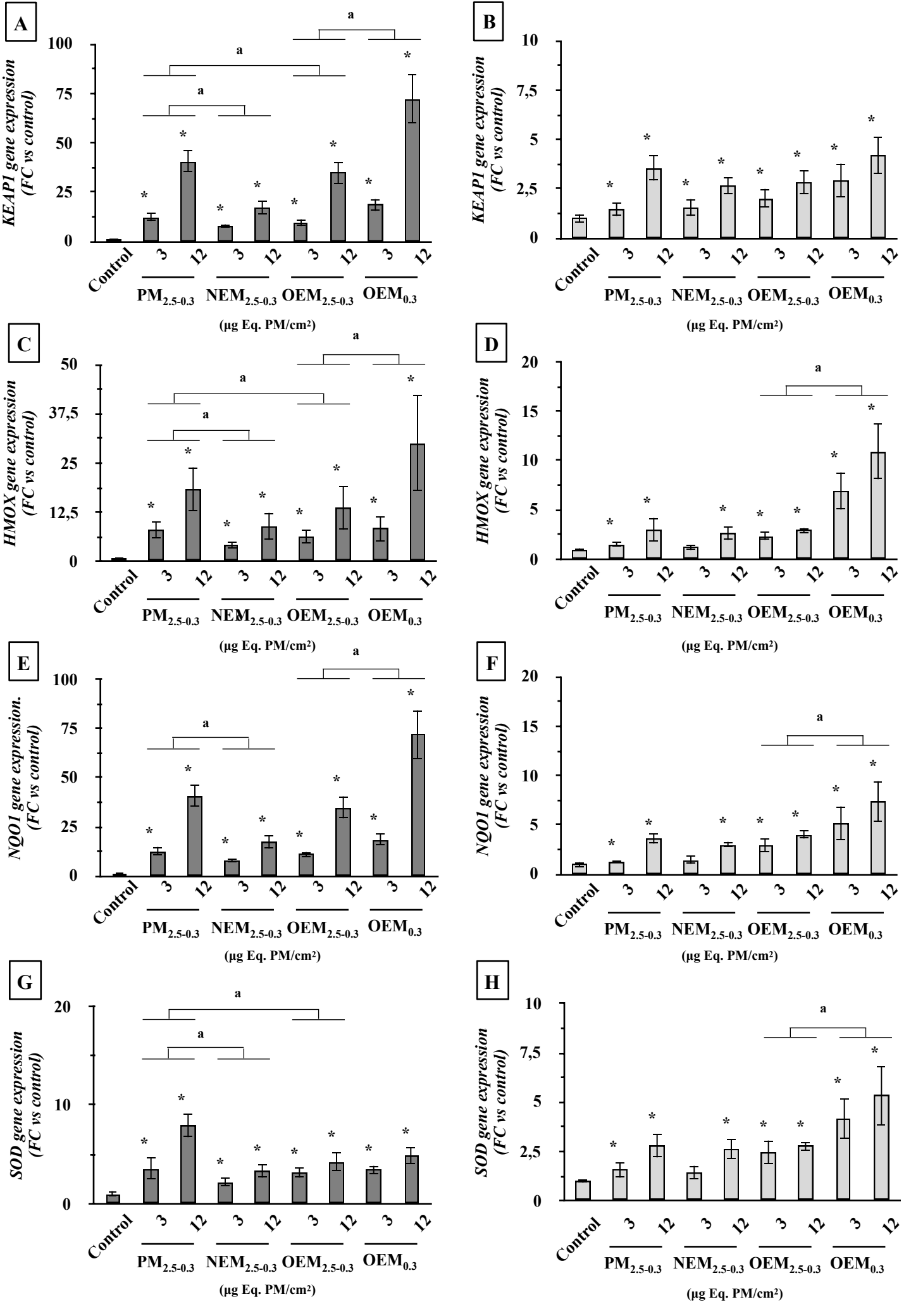
A
B
C
D
E
F
G
H
KEAP1 gene expression (FC vs control)
HMOX gene expression (FC vs control)
NQO1 gene expression. (FC vs control)
SOD gene expression (FC vs control)
Control
3
12
PM2.5-0.3
NEM2.5-0.3
OEM2.5-0.3
OEM0.3
(µg Eq. PM/cm²)
a
*

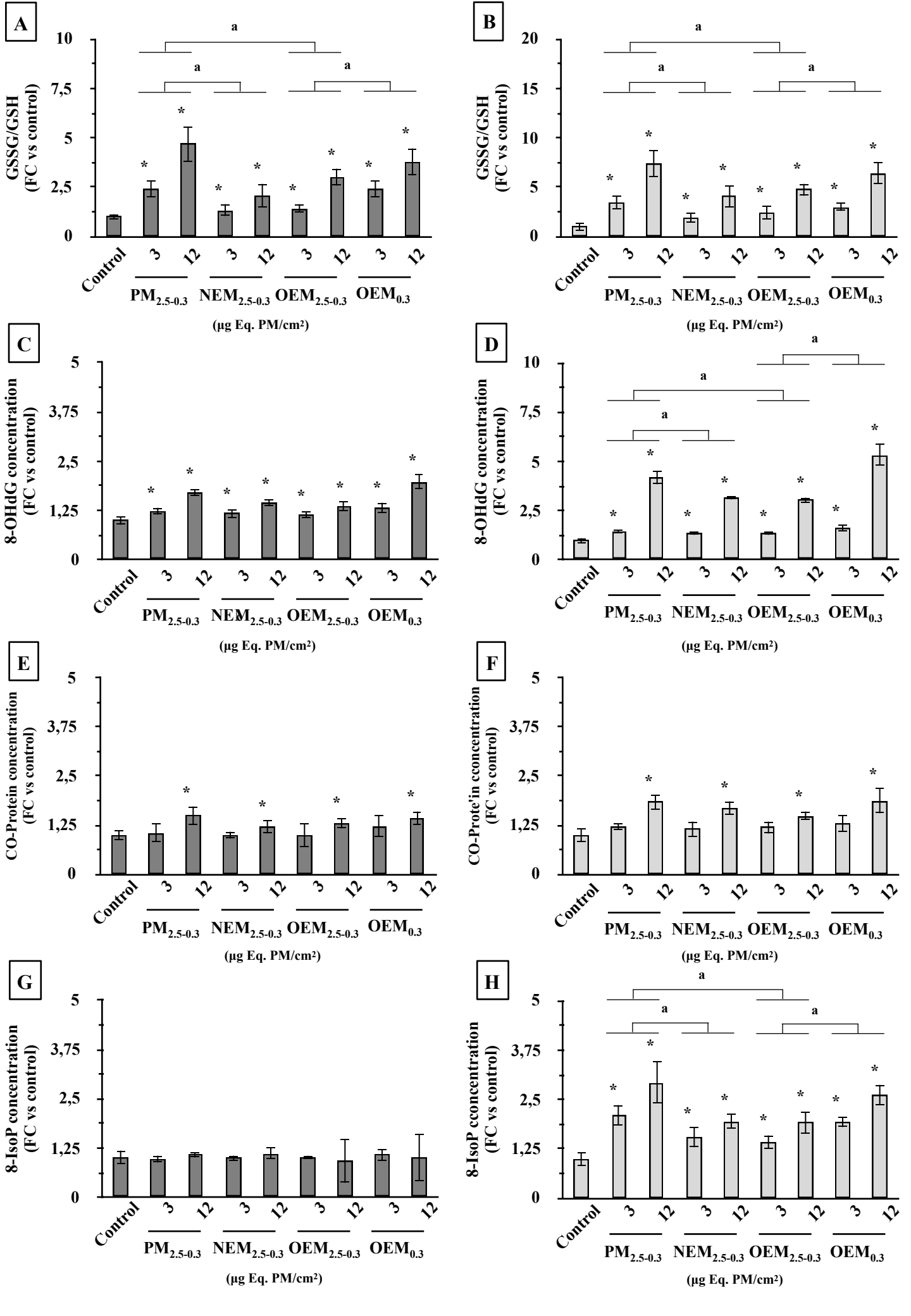
A
B
C
D
E
F
G
H
GSSG/GSH (FC vs control)
8-OHdG concentration (FC vs control)
CO-Protein concentration (FC vs control)
CO-Protein cconcentration (FC vs control)
8-IsoP concentration (FC vs control)
8-IsoP cconcentration (FC vs control)
Control
3
12
PM2.5-0.3
NEM2.5-0.3
OEM2.5-0.3
OEM0.3
(µg Eq. PM/cm²)
a
*

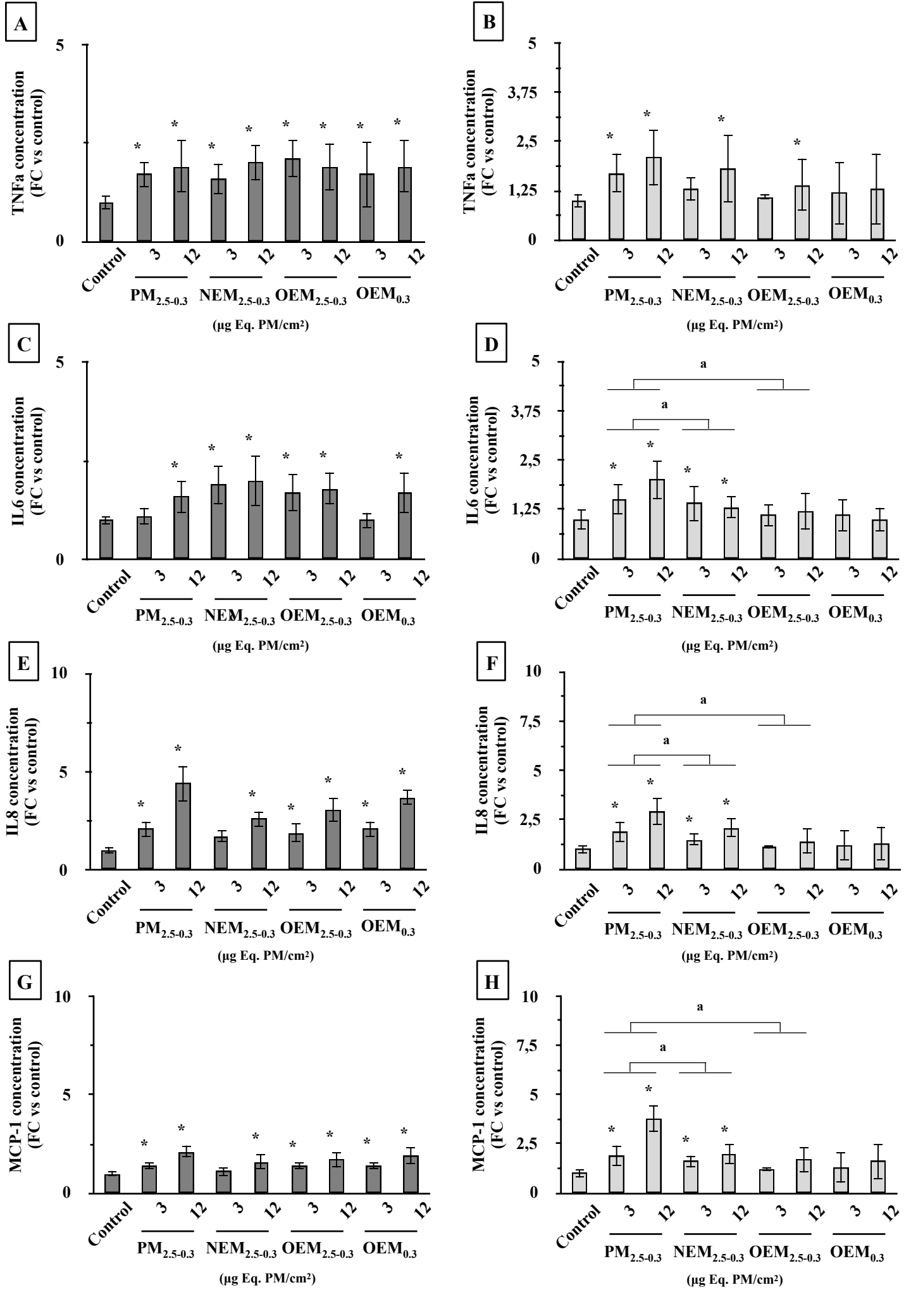
A
B
C
D
E
F
G
H
TNFa concentration (FC vs control)
IL6 concentration (FC vs control)
IL8 concentration (FC vs control)
MCP-1 concentration (FC vs control)
Control
3
12
PM2.5-0.3
NEM2.5-0.3
OEM2.5-0.3
OEM0.3
(µg Eq. PM/cm²)
a

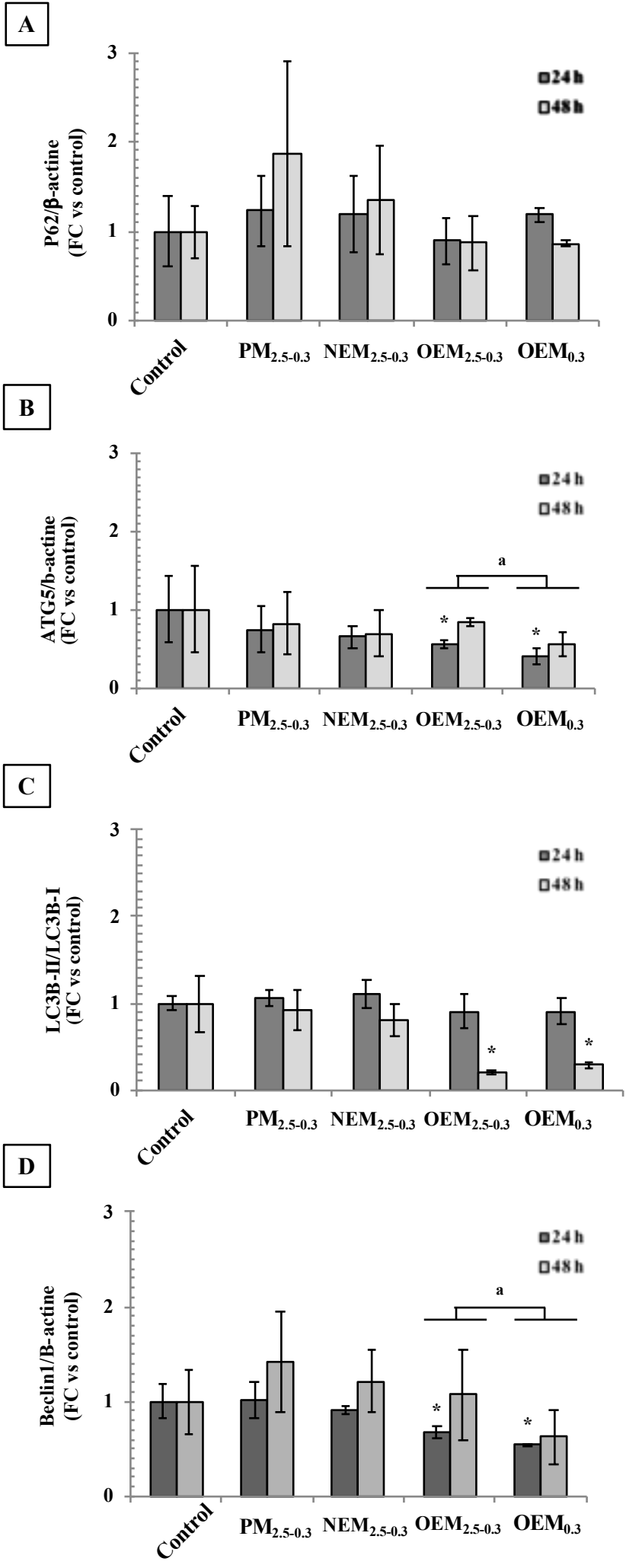
A
P62/β-actine (FC vs control)
24 h
48 h
Control
PM2.5-0.3
NEM2.5-0.3
OEM2.5-0.3
OEM0.3
B
ATG5/b-actine (FC vs control)
a
C
LC3B-II/LC3B-I (FC vs control)
D
Beclin1/B-actine (FC vs control)

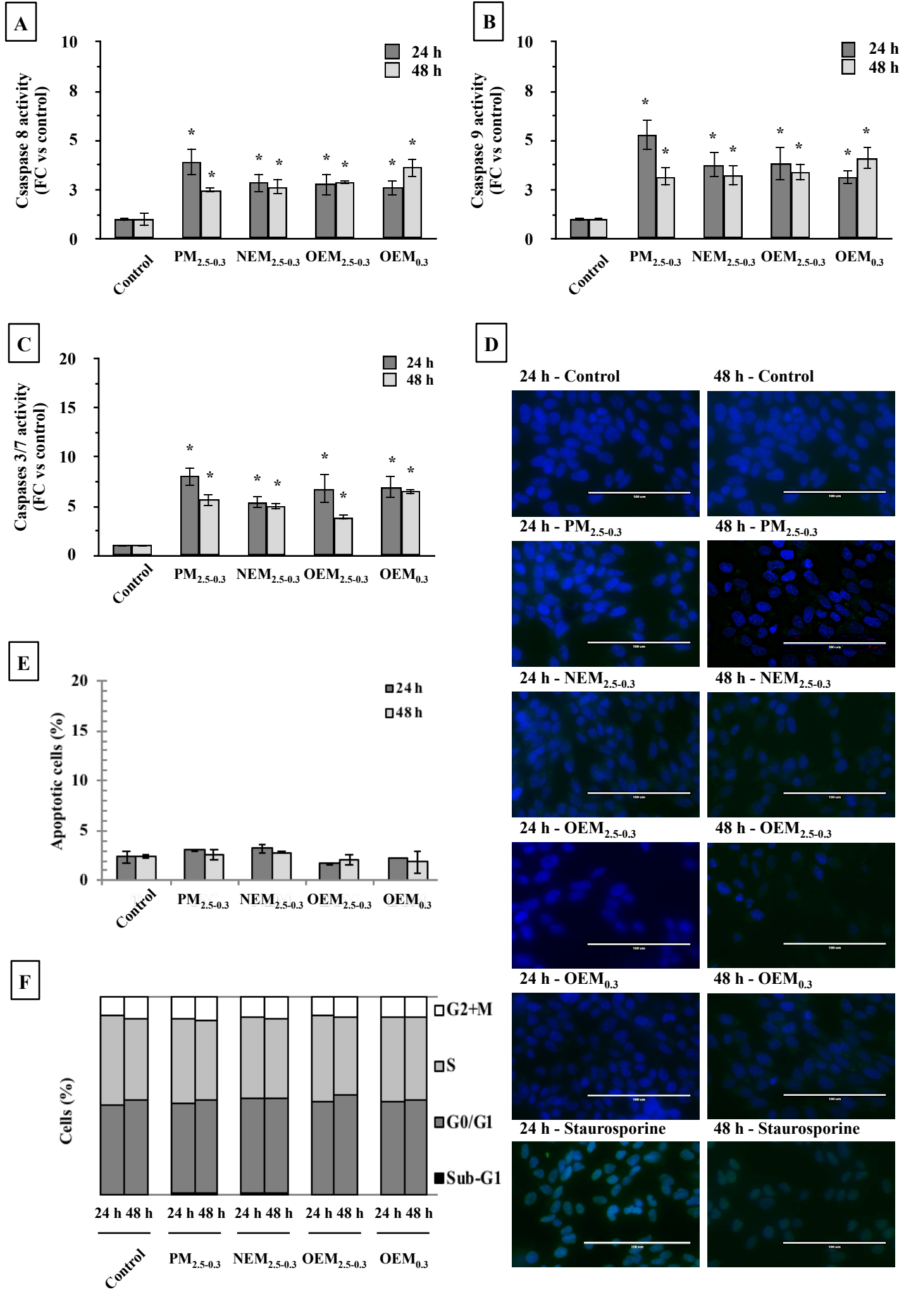
A
Csaspase 8 activity (FC vs control)
24 h
48 h
Control
PM2.5-0.3
NEM2.5-0.3
OEM2.5-0.3
OEM0.3
B
Csaspase 9 activity (FC vs control)
C
Caspases 3/7 activity (FC vs control)
D
24 h - Control
48 h - Control
24 h - PM2.5-0.3
48 h - PM2.5-0.3
24 h - NEM2.5-0.3
48 h - NEM2.5-0.3
24 h - OEM2.5-0.3
48 h - OEM2.5-0.3
24 h - OEM0.3
48 h - OEM0.3
24 h - Staurosporine
48 h - Staurosporine
E
Apoptotic cells (%)
F
Cells (%)
G2+M
S
G0/G1
Sub-G1
24 h 48 h

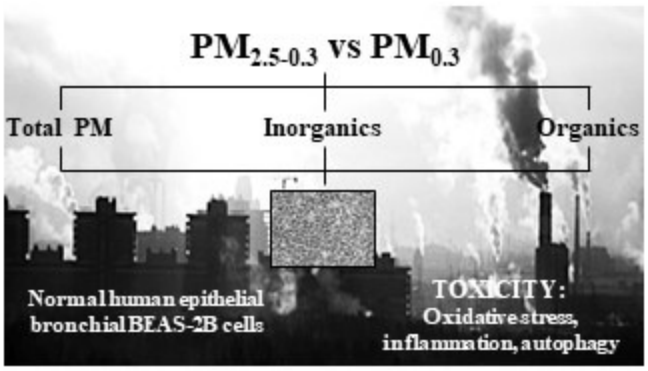
PM2.5-0.3 vs PM0.3
Total PM
Inorganics
Organics
Normal human epithelial bronchial BEAS-2B cells
TOXICITY:
Oxidative stress, inflammation, autophagy